

Distillation Policy Optimization

Jianfei Ma

Northwestern Polytechnical University
School of Mathematics and Statistics
matrixfeeny@gmail.com

Abstract

On-policy algorithms are supposed to be stable, however, sample-intensive yet. Off-policy algorithms utilizing past experiences are deemed to be sample-efficient, nevertheless, unstable in general. Can we design an algorithm that can employ the off-policy data, while exploit the stable learning by sailing along the course of the on-policy walkway? In this paper, we present an actor-critic learning framework that borrows the distributional perspective of interest to evaluate, and cross-breeds two sources of the data for policy improvement, which enables fast learning and can be applied to a wide class of algorithms. In its backbone, the variance reduction mechanisms, such as unified advantage estimator (UAE), that extends generalized advantage estimator (GAE) to be applicable on any state-dependent baseline, and a learned baseline, that is competent to stabilize the policy gradient, are firstly put forward to not merely be a bridge to the action-value function but also distill the advantageous learning signal. Lastly, it is empirically shown that our method improves sample efficiency and interpolates different levels well. Being of an organic whole, its mixture places more inspiration to the algorithm design. Code is available at <https://github.com/MagiFeeney/DPO>.

1. Introduction

Deep model-free reinforcement learning (RL) is a promising solution method that budes the complexity of a rich array tasks with autonomy. Its success prevails by grace of the several breakthroughs regarding to the adaptation with the neural networks. Reminiscent of the Deep Q-learning (Mnih et al., 2013), the replay buffer is first proposed to decorrelate the experience, and reuse them to allow stabler weight updates repeatedly. Its successors such as DDPG (Lillicrap et al., 2016), TD3 (Fujimoto et al., 2018), and SAC (Haarnoja et al., 2018a), with a set of modifications,

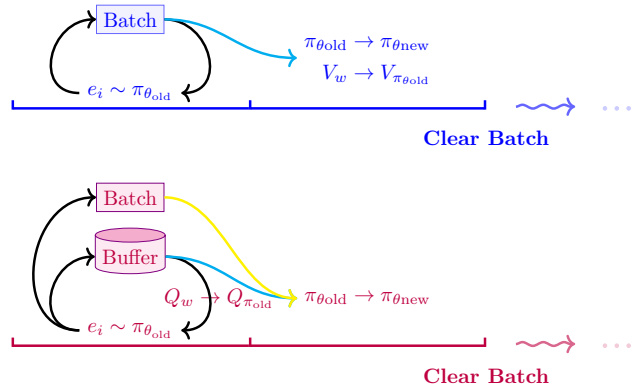


Figure 1. Training procedure comparison between PPO and DPO, in which $e_i = (s_i, a_i, r_i, s'_i)$. Top: PPO; Bottom: DPO.

achieves scalable and notable performance. While those popular algorithms has their own scope that works on, they are categorized as off-policy algorithms, of which one advantage would be the great sample efficiency profited by the replay buffer. Nevertheless, when combined with the off-policy learning, it can also be unstable due to the bootstrapping and the bias incurred. At the other end, A2C, as an on-policy algorithm, is easy-to-use and can learn fast, indicating the vital importance of reducing the variance of the policy gradient by virtue of a baseline function. More advanced algorithms such as TRPO (Schulman et al., 2015), and later, PPO (Schulman et al., 2017), stemming from the concept of keeping the policy to be updated as similar to the sampling policy as possible, can reuse the collected data (or a batch) multiple times. Those algorithms are generally more stable since they don't trigger out the deadly triad (van Hasselt et al., 2018), though, sample-intensive still. Reviewing those two classes, we are aimed to develop a stable and sample-efficient algorithm, by drawing on advantages of both, while following the walkway of the on-policy algorithms.

The first challenge would be how we can bridge the traditional use of value function to the more potential action-value function for incorporating off-policy data. This trans-

fer makes Generalized Advantage Estimator (GAE) (Schulman et al., 2016) no longer applicable, since it only focuses on the value function. However, for algorithms that utilize a batch of data, it is crucial for reducing the variance of the gradient estimate, and the effect could be more amplified by introducing a baseline function. In a conventional use, as the value function is naturally obtainable, it is widely used to compensate for noisiness of the policy gradient. However, as (Ilyas et al., 2020) indicates, this typically approximated one is not so satisfactory as expected. Considering those two folds, we are firstly able to extend GAE to be applicable on any state-dependent baseline, and even more, the appraisal – action-value function. What method we proposed that – UAE, is capable of dealing with different baselines, even injected with the perturbation, while its counterpart fails. On top of that, inspired from the form of the optimal baseline (Greensmith et al., 2001) (usually intractable), we propose to learn a baseline function with a parameterized multiplier adjoint the action-value function. It is trained with off-policy data, therefore can be incorporated with the off-policy policy gradient, not merely on the on-policy counterpart.

Based on the variance reduction mechanisms, we explore to enable fast, stable and efficient learning on both policy evaluation and improvement. In a “deep” sense, the fitted Q-iteration (FQI) (Ernst et al., 2005) (Fan et al., 2020) is commonly used for policy evaluation by numerous algorithms based on the mean squared error loss (MSE), with varying targets. It can either be Monte-Carlo estimate, or temporal-difference target. The truncated version of the former is widely used in on-policy algorithms, however, whose issue of high variance appeals to an effective way for variance reduction. And the latter can either be deterministic (Mnih et al., 2013) or stochastic (Haarnoja et al., 2018a), which utilizes the replayed experiences to allow ample predictions. As Bellman equations are held for any transition, it is natural to think can we efficiently predict the appraisal of interest for on-policy algorithms in an off-policy way. A possible solution as briefly illustrated in Figure 1, repeatedly imitates the Bellman equation through distributional learning. In contrast, for such a long-horizon problem, MSE would fail at the prediction on both rollouts and the unseen data, even equipped with the clipped double Q technique (Fujimoto et al., 2018). At the policy improvement stage, we follow a direction interpolating the policy gradient endowed by any on-policy algorithm and the gradient of the Kullback–Leibler divergence (KL) between current policy and the positive advantage (distilled by the baseline function). While the negative part is strictly canceled out, it is beneficial for a stable learning and inherently encourages exploration.

In this paper, we arrive at a general learning framework, namely Distillation Policy Optimization (DPO), which can

be readily applied on the A2C, TRPO and PPO, outperforming on most continuous benchmark tasks. We will address the components mentioned earlier at a time, and give the theoretical insight for a better understanding. Empirically, we verified the effectiveness of our method with statistical measures, and the evidence shows that DPO can be a strong competitor to the current state-of-the-art.

2. Preliminaries

2.1. Notation

We consider an infinite-horizon discounted MDP, which formulates how the agent interacts with the environment dynamics. It can be defined by a tuple $\mathcal{M} = (\mathcal{S}, \mathcal{A}, P, r, \rho_0, \gamma)$. Reinforcement learning aims to solving a sequential problem. Being at the state $s_t \in \mathcal{S}$, the agent takes an action $a_t \in \mathcal{A}$ according to some policy π , which assigns a probability $\pi(a_t|s_t)$ to the choice. After the environment receives a_t , it emits a reward r_t , and sends the agent to a new state $s_{t+1} \sim P(s_{t+1}|s_t, a_t)$. We assume that the reward signal is bounded by some constant C_r . Following this procedure, we can collect a trajectory $\tau = (s_0, a_0, s_1, a_1, \dots)$, where s_0 is sampled from the distribution of the initial state ρ_0 . The ultimate goal of the agent is to maximize the expected discounted reward $\eta(\pi) = \mathbb{E}_\tau \left[\sum_{t=0}^{\infty} \gamma^t r_t \right]$, with a discount factor $\gamma \in [0, 1)$. We also define the unnormalized discounted state visitation distribution (improper) as $\rho_\pi = \sum_{t=0}^{\infty} \gamma^t P(s_t = s | \rho_0, \pi)$, and $d_\pi(s, a) = \rho_\pi(s) \pi(a|s)$, corresponding to the state-action one. Whenever noticed, the policy will be parameterized as π_θ , sometimes abbreviated as π for simplicity’s sake. Thus the objective turns out to be $\eta(\theta)$. We declare that we are using the l^2 -norm variance of a random vector X , that is, $\mathbb{V}[X] = \mathbb{E}[\|X - \mathbb{E}[X]\|_2^2]$ or equivalently, the trace of the covariance matrix $\text{tr}[\text{cov}[X]] = \mathbb{E}[(X - \mathbb{E}[X])^T (X - \mathbb{E}[X])]$.

2.2. Policy Gradient

The policy gradient (Sutton et al., 1999) is formally stated as

$$\nabla_\theta \eta(\theta) = \mathbb{E}_{s \sim \rho_{\pi_\theta}, a \sim \pi_\theta} [\nabla_\theta \log \pi_\theta(a|s) Q^{\pi_\theta}(s, a)] \quad (1)$$

In practice, incorporating a state-dependent baseline function $b(s)$ can not only reduce the variance drastically but also not intervene the expectation (Greensmith et al., 2001). Combine it together, we have

$$\begin{aligned} \nabla_\theta \eta(\theta) &= \mathbb{E}_{s \sim \rho_{\pi_\theta}, a \sim \pi_\theta} [\nabla_\theta \log \pi_\theta(a|s) (Q^{\pi_\theta}(s, a) - b(s))] \\ &= \mathbb{E}_{s \sim \rho_{\pi_\theta}, a \sim \pi_\theta} [\nabla_\theta \log \pi_\theta(a|s) A^{\pi_\theta, b}(s, a)] \end{aligned} \quad (2)$$

2.3. Optimal Baseline

Optimal baseline can be derived by obtaining the fixed point of the variance of Equation 2

$$b^*(s) = \frac{\mathbb{E}_{\pi_\theta}[u_\theta(s, a)^\top u_\theta(s, a) Q^{\pi_\theta}(s, a) | s]}{\mathbb{E}_{\pi_\theta}[u_\theta(s, a)^\top u_\theta(s, a) | s]} \quad (3)$$

where $u_\theta(s, a) = \nabla_\theta \log \pi_\theta(a | s)$. Its derivation can be found at Appendix A.1.

However, this baseline is rarely used in practice, because it is extremely demanding for computing the $u_\theta(s_t, a_t)$ for each time step of the available data.

2.4. Distributional Reinforcement Learning

Distributional reinforcement learning (Bellemare et al., 2017) abstracts the appraisal $Q^\pi(s, a)$ as a distribution $Z^\pi(s, a)$, whose expectation corresponds to the actual value of Q . In this perspective, the Bellman expectation operator is reloaded as

$$\begin{aligned} \mathcal{T}^\pi Z(s, a) & \stackrel{D}{=} r(s, a) + \gamma Z(s', a') \\ s' & \sim P(\cdot | s, a), a' \sim \pi(\cdot | s') \end{aligned} \quad (4)$$

where the equality is held under probability laws.

3. Unified Advantage Estimator

The quality of the policy gradient is determined by that of the advantage estimate and the data available at hand. For the batch learning, the advantage function of Equation 2 is often approximated by the data with a fixed-length segment. When function approximation is involved, it has to approximate the true appraisal Q^π or V^π by Q or V respectively, and a baseline for variance reduction. In this event, GAE, that introduces an additional discount parameter λ , can further reduce the variance of the policy gradient estimate. Nevertheless, its scope is only on the case where the $b(s_t) = V(s_t)$, and $Q(s_t, a_t) \approx r_t + \gamma V(s_{t+1})$, by solely using the value function V , which limits its extensive use. We will relax it for the both parts, that is, $Q(s_t, a_t) \approx r_t + \gamma Q(s_{t+1}, a_{t+1})$, and $b(s_t)$ for any form. Like GAE, we can also define the TD residual $\delta_t = r_t + \gamma \Psi_{t+1} - b(s_t)$, where $\Psi_{t+1} = Q(s_{t+1}, a_{t+1})$ or $V(s_{t+1})$. Additionally, a correction term $z_t = \Psi_t - b(s_t)$ is defined. When the corrected value of Ψ_t is attained, we have the following proposition

Proposition 3.1. *For any $n \in \mathbb{N}^+$, $A_t^{(n)}$ is an unbiased estimator of $A_t^{\pi, b}$, where*

$$A_t^{(n)} = \delta_t + \sum_{l=1}^{n-1} \gamma^l (\delta_{t+l} - z_{t+l}) \quad (5)$$

Algorithm 1 Unified Advantage Estimator

Input: γ, λ , Batch size T , rewards r , Q values Q , baselines b , dones d
Initialize uae = 0
for $t = T - 1, T - 2, \dots, 0$ **do**
 $\delta = r_t + \gamma Q_{t+1}(1 - d_{t+1}) - b_t$
 $z = Q_t - b_t$
 discounted uae = $\gamma \lambda (1 - d_{t+1})$ uae
 $A_t = \delta + \text{discounted uae}$
 uae = $(\delta - z) + \text{discounted uae}$
end for
return advantages A

Be that as it may, in practice, Ψ_t is approximated and thus the A_t^n is referenced as \hat{A}_t^n . By telescoping on λ^n , we deliver the UAE as (see Appendix B)

$$\hat{A}_t^{\text{UAE}(\gamma, \lambda)} = \delta_t + \sum_{l=1}^{\infty} (\gamma \lambda)^l (\delta_{t+l} - z_{t+l}) \quad (6)$$

It is worth noting that if we set $\Psi_{t+1} = V(s_{t+1})$ and $b(s_t) = V(s_t)$, then we have the GAE exactly. To tell this, note that $z_t = \Psi(s_t) - b(s_t) = 0$, thus it reduces to the formula of the GAE. That is to say, if we set the same seeds for experiments, we will get the same reward for UAE and GAE. However, it has a far-reaching use since we are free to choose any state-dependent baseline, and extend it to the action-value function. Figure 2(b) illustrates that even if we inject random noise into the baseline, or leave it aside (zero baseline), UAE is robust to those changes, where its counterpart Monte-Carlo estimate fails. A truncated version of such an estimator is depicted in Algorithm 1.

Similar to GAE, UAE also has two special cases, come by setting $\lambda = 0$ and $\lambda = 1$.

$$\begin{aligned} \text{UAE}(\gamma, 0) : \hat{A}_t &= r_t + \gamma \Psi_{t+1} - b(s_t) \\ \text{UAE}(\gamma, 1) : \hat{A}_t &= \sum_{l=0}^{\infty} \gamma^l r_{t+l} - b(s_t) \end{aligned} \quad (7)$$

Any intermediate value of λ would interpolate those two ends, trading-off the bias and variance. Normally, choosing λ close to 1 could introduce some bias but reduce the variance significantly.

However, we argue that the full capability of UAE requires a good baseline, once it is chosen we cannot touch the innards of the set of TD residuals anymore. This can be more amplified for the first term, which neither GAE or UAE has a control of. As the variance decomposition shows, with $\chi_l = u_\theta(s_{t+l}, a_{t+l})(\delta_{t+l} - z_{t+l})$, $l \geq 0$ and $z_{t+l} = 0$ if

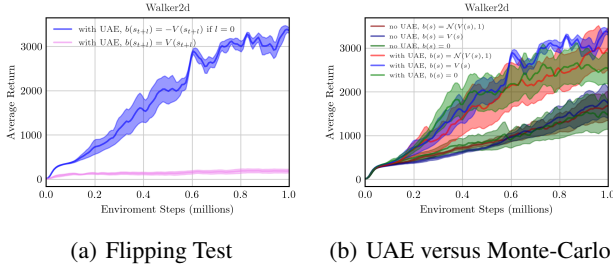


Figure 2. Comparison of the effect of UAE by modifying partially or turning it off totally on top of the PPO. **Left**: flip the sign of the first-term baseline; **Right**: comparison between UAE and Monte-Carlo estimate with constant, perturbed and value baseline.

$l = 0$

$$\begin{aligned} \mathbb{V}[u_\theta(s_t, a_t) \hat{A}_t^{\text{UAE}(\gamma, \lambda)}] &= \mathbb{V}[\chi_0] \\ &+ \sum_{l=1}^{\infty} (\gamma \lambda)^{2l} \mathbb{V}[\chi_l] \\ &+ 2 \sum_{0 \leq i < j} (\gamma \lambda)^{i+j} \text{cov}(\chi_i, \chi_j) \end{aligned} \quad (8)$$

even though the exponentially discounting successfully shrinks the temporal spread when $l > 0$, it has no control of that at $l = 0$. As indicated in the Figure 2(a), even if we just flip the sign of the such a term, while remain the subsequent terms unchanged, it can bring out a drastical drop.

In next section, we aim to learning a more flexible baseline, which can even be incorporated in the off-policy learning later on.

4. Learn a Baseline

As previously mentioned, obtaining the $u_\theta(s, a)$ can be exhausting. This overhead is inevitable especially when the batch is large. As a consequence, the optimal baseline (Equation 3) is difficult to reach. And in practice, due to the estimation error, the value function as a baseline is not as satisfactory as its true value (Ilyas et al., 2020). We are in an attempt to set aside that overhead, and improve the quality of the baseline. By observing the structure of the optimal baseline, we define that

$$\begin{aligned} \tilde{\pi}(a|s) &= \frac{\pi(a|s) u_\theta(s, a)^T u_\theta(s, a)}{\mathbb{E}_\pi[u_\theta(s, a)^T u_\theta(s, a)|s]} \\ l(s, a) &= \frac{u_\theta(s, a)^T u_\theta(s, a)}{\mathbb{E}_\pi[u_\theta(s, a)^T u_\theta(s, a)|s]} \end{aligned} \quad (9)$$

then we can rewrite the optimal baseline as:

$$b^*(s) = \mathbb{E}_\pi[Q^\pi(s, a)|s] \quad (10)$$

Using the importance sampling, we have:

$$\begin{aligned} b^*(s) &= \mathbb{E}_\pi\left[\frac{\tilde{\pi}(a|s)}{\pi(a|s)} Q^\pi(s, a)|s\right] \\ &= \mathbb{E}_\pi[l(s, a) Q^\pi(s, a)|s] \end{aligned} \quad (11)$$

We can directly parameterize the $l(s, a)$, or, alternatively, introduce a ‘‘residual’’ term $r_\psi(s, a)$ to reformulate the $l(s, a)$ as $1 + r_\psi(s, a)$, since $\mathbb{E}_\pi[l(s, a)] = 1$. This transformation would induce a symmetric behavior for $r_\psi(s, a)$, which is favored by the neural network. It translates to approximate the Equation 11 as:

$$b_\psi^\pi(s) = \mathbb{E}_\pi[(1 + r_\psi(s, a)) Q^\pi(s, a)|s] \quad (12)$$

When a state s is given, we sample m actions a_1, a_2, \dots, a_m from the $\pi(\cdot|s)$ to approximate this parameterized baseline. In the hope that Q_w is a good approximation to the Q^π , the approximate baseline has a form of:

$$\hat{b}_\psi^\pi(s) = \frac{1}{m} \sum_{i=1}^m (1 + r_\psi(s, a_i)) Q_w(s, a_i) \quad (13)$$

This can be viewed as sampling with replacement, each $Q_w(s, a_i)$ has nothing to do with the actual action a .

We then construct a magnitude free objective to represent the amount of the variance associated with the approximate baseline.

$$\mathcal{L}(\psi) = \mathbb{E}_{(s,a) \sim d_\mu} [(Q_w(s, a) - \hat{b}_\psi^\pi(s))^2] \quad (14)$$

For the N th update, $d_\mu(s, a) = \frac{1}{N} \sum_{i=1}^N d_{\pi_i}(s, a)$. With the data from the replay buffer \mathcal{D} evenly collected by each policy with a fixed-length segment, we can approximate this surrogate function.

At first glance it would be suspicious for the stream of data trained on, however, this subtle difference allows the baseline to be incorporated into the off-policy policy gradient, not merely for the on-policy policy gradient.

Assumption 4.1. $\sup_s \mathbb{E}_\pi[\nabla_\psi r_{\psi^*} Q^\pi]$ is bounded by some constant C_g

Assumption 4.2. $\sup_{s,a} |r_{\psi^*}(s, a)|$ is bounded by some constant \tilde{C}

where ψ^* is obtained by minimizing Equation 14.

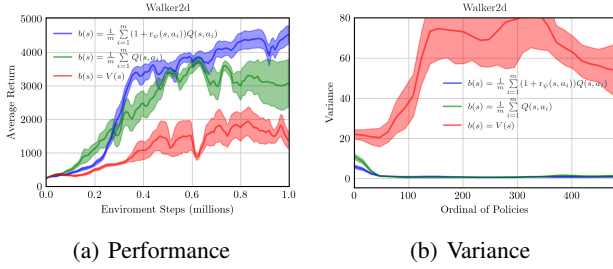


Figure 3. Comparison between three baselines. **Left**: performance on the Walker2d task; **Right**: variance of each baseline estimated over the rollouts.

Theorem 4.3. ϵ -stationary point Under Assumption 4.1, for the current policy π , along with its predecessors $\{\pi_i\}_{i=1}^{N-1}$, if for any $s \in \mathcal{S}$, $\sup_i D_{TV}(\pi_i || \pi) < \frac{\epsilon}{4N}$ and $\mathbb{E}_{\pi}[|r_{\psi^*}(s, a)|] < \frac{\epsilon}{2N}$, then $|\nabla_{\psi} \mathcal{L}(\psi^*)| < \frac{2C_r C_g}{1-\gamma} \epsilon$.

Corollary 4.4. Under Assumption 4.2, for any successor policy $\tilde{\pi}$ of π , if $\sup_s D_{KL}(\tilde{\pi} || \pi) < \frac{\epsilon}{4}$, then

$$\mathbb{E}_{d_{\mu}} [(Q_w(s, a) - \hat{b}_{\tilde{\psi}^*}(s))^2] \leq 2\mathcal{L}(\psi^*) + \frac{2((\tilde{C} + 1)C_r)^2}{(1-\gamma)^2} \epsilon \quad (15)$$

The Corollary 4.4 states that for a baseline that induced by the policy π , any policy ahead of it can have a considerably small magnitude-free variance, as long as not being too far away from the origin. This could be the case such as for trust-region methods, TRPO and PPO. Efficiently utilizing such a baseline can reduce the overall variance of the policy gradients, and thus smoothing out the learning process. We in advance made comparison with different baseline functions, such as baseline $V(s)$ and with residual $r = 0$, which is presented in the Figure 3.

5. Practical Algorithm

Draw attention back on the practical algorithm, with off-policy data incorporated, its designing has two challenges, corresponding to either policy evaluation or improvement. First, how to stably, efficiently, and accurately evaluate the true appraisal while generalize well during training, which is posed as a challenge in (Fujimoto et al., 2022) for standard FQI methods? Second, how to boost the data efficiency by interpolating the off-policy policy gradient, while not intervene the on-policy policy gradient too much? In next sessions, we will address those problems with distributional learning perspective and projected advantageous policy gradient.

5.1. Policy Evaluation: Distributional Regression

Distributional learning provides us a richer set of predictions, bearing a surface resemblance to the value perspective. We will rely on such a representation by imitating the distributional Bellman operator as shown in Equation 4, but not concern the contraction property in the distributional sense. It is only of interest to consider the contraction property in the expectation sense, which should be representative to the true appraisal Q^{π} . As following lemma shows, such a property is as desired

Lemma 5.1. Consider two value distributions $Z_1, Z_2 \in \mathcal{Z}$, it contracts in both expectation and variance

$$\begin{aligned} \|\mathbb{E}\mathcal{T}^{\pi} Z_1 - \mathbb{E}\mathcal{T}^{\pi} Z_2\|_{\infty} &\leq \gamma \|\mathbb{E}Z_1 - \mathbb{E}Z_2\|_{\infty} \\ \|\mathbb{V}\mathcal{T}^{\pi} Z_1 - \mathbb{V}\mathcal{T}^{\pi} Z_2\|_{\infty} &\leq \gamma^2 \|\mathbb{V}Z_1 - \mathbb{V}Z_2\|_{\infty} \end{aligned} \quad (16)$$

This contraction property is essential for learning the appraisal accurately, as it not only contracts in mean but also quicker in variance. As the variance diminishes in the limit, it turns out to be nearly deterministic, which would coincide the behavior of the standard Bellman operator in the limit. Based on Lemma 5.1, we further restrict ourselves to the class of normal distributions, due to its simplicity and intuitive interpretation. It will perform on the KL divergence loss repeatedly by using replayed experiences

$$\mathcal{L}(w) = \mathbb{E}_{(s, a, r, s') \sim D} [D_{KL}(r + \gamma Z_{\bar{w}}(s', a') || Z_w(s, a))] \quad (17)$$

where $a' \sim \pi(\cdot | s')$, and $Z_{\bar{w}}$ is the target network, commonly used in the off-policy learning to stabilize the neural network.

It bears a close relationship to the MSE loss, which is stated in the following proposition

Proposition 5.2. Let σ_1 and σ_2 be constantly equal as σ , then KL divergence loss is equivalent to the MSE loss scaled by σ^2 .

It is beneficial to choose the KL divergence loss, as it encompasses the uncertainty directly controlled by the parameter σ . Mutually adjusted by the discrepancies, it is proportional to

$$\begin{aligned} \Delta\sigma &\propto (\sigma_1^2 - \sigma_2^2(\zeta)) + (\mu_1 - \mu_2(\phi))^2 \\ \Delta\mu &\propto (\mu_1 - \mu_2(\phi)) \end{aligned} \quad (18)$$

where ϕ and ζ are a pair of parameters of μ and σ , if there are shared parameters, we can union all the parameters and flatten them to a vector, and fill zeros for those segments that μ or σ don't belong to.

An informal interpretation would be that such a loss nudges the mean values to get closer, and in the meantime, keeps track of the discrepancies of both variance and mean value. Once the difference between two mean values becomes

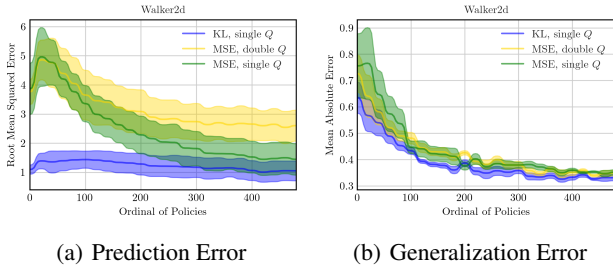


Figure 4. Comparison between **KL divergence with single Q** , **MSE with single Q** and additionally **MSE with double Q** . **Left**: root mean squared error (RMSE) between $\mathbb{E}[r + \gamma Z_{\bar{w}}(s', a')]$ and $\mathbb{E}[Z_w(s, a)]$ averaged on the rollouts; **Right**: mean absolute error (MAE) between the true value Q^π and the fitted value Q_w , averaged on the test data sampled from the current policy π .

large, the uncertainty goes up, which informs it to be incentive in the next cycle. If the difference is small, then it will be more confident by shrinking variance close to the target variance. Compared with the MSE loss, it is also computationally efficient, but updates more carefully, and can generalize well during training, while its counterpart suffers from overfitting and overestimation bias. Even when the clipped double Q technique (Fujimoto et al., 2018) is replenished, it can still fail at the long-horizon scenario. The comparison is presented in the Figure 4, which indicates that the KL divergence can stand out from both prediction online and generalization during training.

5.2. Policy Improvement: Advantageous Interpolation

We seek to incorporate the off-policy policy gradient into the on-policy policy gradient so as to enable faster learning, boost sample efficiency and encourage exploration. The off-policy policy gradient shouldn’t be dominant, in turn it serves to squeeze out the informations at hand. One reason that we places the leader position to the other one is that it is generally stabler, able to learn from the latest rollouts. This mixture would be favored since it combines the merit of both worlds. In that vein, we would define the off-policy policy gradient to begin with

$$\mathcal{L}_{\text{off-policy}}(\theta) = -\mathbb{E}_{s \sim \mathcal{D}} \left[D_{\text{KL}}(\pi_\theta(\cdot|s) \parallel \frac{\frac{1}{\alpha} \exp A^+(s, \cdot)}{N(s)}) \right] \quad (19)$$

where $A^+(s, \cdot) = (Q_w(s, \cdot) - b_\psi(s))^+$, is the positive advantage, of which $(x)^+$ stands for $\max(x, 0)$, $N(s)$ is the partition function, and α is the temperature parameter.

It bears similarity to the loss function of SAC, while the difference is that we strictly cancel out the negative part distilled by the learned baseline. When the action is perceived as bad, it will leave away from that choice, but in

a high probability move towards unknown actions, risking to take totally wrong actions. The baseline function can be viewed as a safe belt, which guarantees that the moving direction is only advantageous. But it sees more data, in turn help the “leader” gradient to generalize and retrospect those experiences that would never happen again. Another difference is that, unlike SAC, we use the likelihood ratio gradient estimator (Williams, 1992), rather than the reparameterization trick. Taking gradient of the Equation 19, it has a cleaner expression

$$\nabla_\theta \mathcal{L}_{\text{off-policy}}(\theta) = \mathbb{E}_{s \sim \mathcal{D}, a \sim \pi_\theta} [\nabla_\theta \log \pi_\theta(a|s) (A^+(s, a) - \alpha \log \pi_\theta(a|s))] \quad (20)$$

It increases the probability for those advantageous actions, and regardlessly encourages exploration over all pairs. This is helpful for the actions that is not in the advantageous set, since it yearns to explore more, rather than sets it aside. And a good property of the positive advantage is that it diminishes in the limit under some conditions

Theorem 5.3. *Under Assumption 4.2, for any policy sequence $\{\pi_k\}$ such that its limiting point π^* lies in the deterministic optimal policy set, if for any $s \in \mathcal{S}$, the limit of $s_k = \sum_{i=1}^{k-1} \int_{\mathcal{A}} (\pi_i - (1 + r_{\psi^*})\pi^*) Q^{\pi^*} da$ exists, then*

$$\limsup_{k \rightarrow \infty} A_k^+ = 0 \quad (21)$$

It indicates that as the positive advantage diminishes, the surrogate reduces to encourage exploration only, when certain conditions meet. A direct consequence is that the expected value of the positive advantage would approach to zero as well. The Figure 5 further supports those claims.

If we combine the off-policy gradient with any on-policy gradient $\nabla \mathcal{L}_{\text{on-policy}}(\theta)$ by an interpolating parameter $\omega \in [0, 1]$, such as A2C, TRPO and PPO, then in the end it will be overwhelmed.

$$\nabla \mathcal{L}(\theta) = \omega \nabla \mathcal{L}_{\text{on-policy}}(\theta) + (1 - \omega) \nabla \mathcal{L}_{\text{off-policy}}(\theta) \quad (22)$$

The complete algorithm is described in the Algorithm 2, as it is integrated best with PPO, we will abuse the notation of DPO(PPO) as DPO, unless otherwise noted.

6. Experiments

As in previous sections we have partially compared and verified the effect of individual component or the claim, in this part, our goal would turn to compare our method with a various competitive algorithms, illustrate the network architecture, and understand how the different components contribute to the algorithm. We perform our algorithm on several continuous control tasks from the OpenAI

Algorithm 2 Distillation Policy Optimization

Initialize parameters w, \bar{w}, θ, ψ
for iteration $i \leftarrow 0, 1, \dots, N - 1$ **do**
 for step $t \leftarrow 0, 1, \dots, M - 1$ **do**
 sample action $a_t \sim \pi(\cdot | s_t)$
 observe reward r_t and next state s_{t+1}
 store transition (s_t, a_t, r_t, s_{t+1}) to replay buffer \mathcal{D}
 and batch \mathcal{B}
 sample mini-batch of n transitions (s, a, r, s') from \mathcal{D}
 update critic with $\nabla_w \mathcal{L}(w)$
 update target network $\bar{w} \leftarrow \tau w + (1 - \tau)\bar{w}$
 end for
 for update $l \leftarrow 0, 1, \dots, L - 1$ **do**
 sample mini-batch of n transitions (s, a, r, s') from \mathcal{D}
 update baseline with $\nabla_\psi \mathcal{L}(\psi)$
 end for
 calculate \hat{A} for \mathcal{B} by Algorithm 1
 for epoch $e \leftarrow 0, 1, \dots, E - 1$ **do**
 for mini-batch from \mathcal{B} $k \leftarrow 0, 1, \dots, K - 1$ **do**
 sample mini-batch of n transitions (s, a, r, s')
 from \mathcal{D}
 update policy with $\nabla_\theta \mathcal{L}(\theta)$
 end for
 end for
 reset the batch \mathcal{B}
end for

Gym (Brockman et al., 2016) with the MuJoCo simulator (Todorov et al., 2012).

6.1. Evaluation

Since our algorithm is in a hybrid fashion, the policy that we update would not strictly follow the sampling policy. We thus evaluate our algorithm by executing the mean action with 10 trails, for which we report the averaged episodic reward every 4096 steps. We run each task with 5 random seeds, whose total environment step is 1 million.

As our on-policy learner is PPO, we compare against it to verify whether our method realizes an improvement. We also made comparisons with the state-of-the-art off-policy algorithms, such as SAC (Haarnoja et al., 2018a) that is closely connected with our off-policy policy gradient, and TD3 (Fujimoto et al., 2018) the deterministic variant of the DDPG. All the on-policy algorithms are implemented from OpenAI Baselines (Dhariwal et al., 2017), including A2C, TRPO and PPO. It is implemented with the latest version of SAC with auto-temperature (Haarnoja et al., 2018b), from

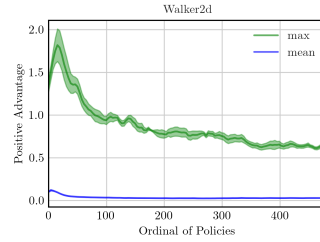


Figure 5. Mean and max value of the positive advantage estimated over the uniformly sampled data from the replay buffer.

the author’s repository¹, and TD3² as well.

The learning curves are presented in the Figure 6. As we can see, DPO can outperform or on-par on most of the tasks, especially the challenging high-dimensional Humanoid task. This great improvement can also be observed on other two variants of DPO i.e. DPO(A2C) and DPO(TRPO), when the on-policy learner is A2C or TRPO (see Appendix I.1).

6.2. Network Architecture

Majority of the DRL algorithms parameterize the policy as a Gaussian distribution, due to its simplicity. However, the boundary effect of it is observed in several works (Chou et al., 2017) (Fujita & Maeda, 2018). And in practice, the action space is usually bounded, thus it is beneficial to parameter our policy as a beta policy. Like (Chou et al., 2017), the shape parameters α, β is forwarded though a fully connected neural network, and converted to the range $[1, \infty)$ by a softplus activation added with a constant 1. For the critic, we parameterize it as a Gaussian distribution, output the mean value though the last layer, and the standard deviation operated by a softplus activation similarly. For the baseline, it is simply a fully connected neural network that outputs the residual term, when approximating the baseline, a constant 1 is added (see Equation 13). All the networks are with 2 hidden layers, and \tanh activation function, each of which has 256 neurons. This architecture is robust to the hyperparameter changes, especially when different on-policy learners are involved.

6.3. Ablation Study

We investigate the contribution of different components to the performance gain, which are: KL divergence loss (section 5.1), UAE (section 3), policy gradient interpolation (section 5.2), learned baseline (section 4), and positive advantage (section 5.2). The counterpart of those components

¹<https://github.com/rail-berkeley/softlearning>

²<https://github.com/sfujim/TD3>

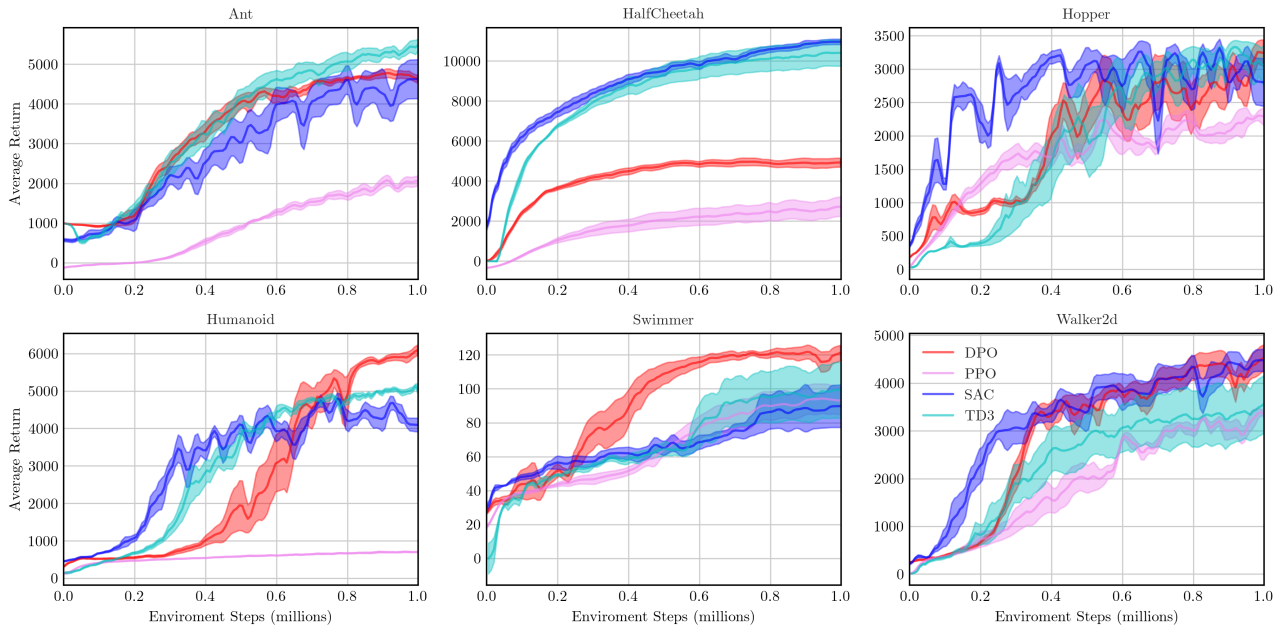


Figure 6. Learning curves on continuous control tasks, averaged over 5 random seeds and shaded with standard error.

would be: MSE with single Q, Monte-Carlo estimate, $\omega = 1$, $r = 1$, and including the negative part. The result is shown in Table 1. The removal of UAE drops down greatest, it indicates the vital importance of reducing the variance of the policy gradients. And removal of other components also has a decrease with varying degree. It justifies the effectiveness of each component, and most of them can be easily transferred into one’s custom algorithm, for practical use.

Table 1. Ablation study on different components. Shorthand INT for policy gradient interpolation, LB for learned baseline, and PA for positive advantage.

METHOD	WALKER2D	HOPPER	ANT
NO-KL	4130± 498	1898± 1352	4527± 429
NO-UAE	1395± 1616	724± 90	908± 75
NO-INT	4014± 1189	1873± 1180	3751± 1184
NO-LB	3104± 1766	2630± 1032	3929± 1336
NO-PA	3561± 1406	2450± 971	4671± 280
DPO	4538± 690	3238± 546	4646± 278

7. Related Work

Variance reduction technique is widely studied in (Green-smith et al., 2001) (Weaver & Tao, 2001) (Schulman et al., 2016). The use of the value function as a baseline is conventionalized, prevailing in on-policy algorithms. However, there is little work that improves on this baseline.

Distributional learning was first structurally studied by (Bellemare et al., 2017), ant later on developed by (Dabney et al., 2018b) (Dabney et al., 2018a). Our algorithm takes advantage of such a distributional perspective for policy evaluation, of which the mean value of the learned distribution is of interest.

Off-policy learning enjoys the data-efficiency especially when combined with the relay buffer, which was firstly proposed in DQN (Mnih et al., 2013). DDPG (Lillicrap et al., 2016) is built upon DQN and DPG (Silver et al., 2014), and TD3 (Fujimoto et al., 2018) focuses on addressing the overestimation bias, while SAC (Haarnoja et al., 2018a) stretches the DDPG style policy gradients out to any tractable stochastic policy.

Policy gradient interpolation was investigated in Q-prop (Gu et al., 2017b) and IPG (Gu et al., 2017a). But they not only fail at policy estimate with a consistent critic, but also overlook the possibility for a more efficient policy evaluation.

Positive advantage can be useful for selecting advantageous actions (van Hasselt, 2012) (Tessler et al., 2019), however, they are not in an attempt to interpolate a richer set of policy gradients. Our design choice is aimed to incorporate the off-policy gradient stably and not mess up the on-policy gradient.

8. Conclusion

In this paper, we proposed a general learning framework, with several components involved. We are the first algorithm that fully connects the on-policy algorithms with the off-policy data. It balances the stable learning and sample efficiency well. We gave theoretical insights and experimental justifications, which would be helpful to understand each part of the algorithm. This kind of mixture would be inspiring for the future algorithm design.

References

- Bellemare, M. G., Dabney, W., and Munos, R. A distributional perspective on reinforcement learning. In Precup, D. and Teh, Y. W. (eds.), *Proceedings of the 34th International Conference on Machine Learning, ICML 2017, Sydney, NSW, Australia, 6-11 August 2017*, volume 70 of *Proceedings of Machine Learning Research*, pp. 449–458. PMLR, 2017. URL <http://proceedings.mlr.press/v70/bellemare17a.html>.
- Brockman, G., Cheung, V., Pettersson, L., Schneider, J., Schulman, J., Tang, J., and Zaremba, W. Openai gym. *CoRR*, abs/1606.01540, 2016. URL <http://arxiv.org/abs/1606.01540>.
- Chou, P., Maturana, D., and Scherer, S. A. Improving stochastic policy gradients in continuous control with deep reinforcement learning using the beta distribution. In Precup, D. and Teh, Y. W. (eds.), *Proceedings of the 34th International Conference on Machine Learning, ICML 2017, Sydney, NSW, Australia, 6-11 August 2017*, volume 70 of *Proceedings of Machine Learning Research*, pp. 834–843. PMLR, 2017. URL <http://proceedings.mlr.press/v70/chou17a.html>.
- Dabney, W., Ostrovski, G., Silver, D., and Munos, R. Implicit quantile networks for distributional reinforcement learning. In Dy, J. G. and Krause, A. (eds.), *Proceedings of the 35th International Conference on Machine Learning, ICML 2018, Stockholm, Sweden, July 10-15, 2018*, volume 80 of *Proceedings of Machine Learning Research*, pp. 1104–1113. PMLR, 2018a. URL <http://proceedings.mlr.press/v80/dabney18a.html>.
- Dabney, W., Rowland, M., Bellemare, M. G., and Munos, R. Distributional reinforcement learning with quantile regression. In McIlraith, S. A. and Weinberger, K. Q. (eds.), *Proceedings of the Thirty-Second AAAI Conference on Artificial Intelligence, (AAAI-18), the 30th innovative Applications of Artificial Intelligence (IAAI-18), and the 8th AAAI Symposium on Educational Advances in Artificial Intelligence (EAAI-18), New Orleans, Louisiana, USA, February 2-7, 2018*, pp. 2892–2901. AAAI Press, 2018b. URL <https://www.aaai.org/ocs/index.php/AAAI/AAAI18/paper/view/17184>.
- Dhariwal, P., Hesse, C., Klimov, O., Nichol, A., Plappert, M., Radford, A., Schulman, J., Sidor, S., Wu, Y., and Zhokhov, P. Openai baselines. <https://github.com/openai/baselines>, 2017.
- Ernst, D., Geurts, P., and Wehenkel, L. Tree-based batch mode reinforcement learning. *Journal of Machine Learning Research*, 6, 2005.
- Fan, J., Wang, Z., Xie, Y., and Yang, Z. A theoretical analysis of deep q-learning. In Bayen, A. M., Jadbabaie, A., Pappas, G. J., Parrilo, P. A., Recht, B., Tomlin, C. J., and Zeilinger, M. N. (eds.), *Proceedings of the 2nd Annual Conference on Learning for Dynamics and Control, L4DC 2020, Online Event, Berkeley, CA, USA, 11-12 June 2020*, volume 120 of *Proceedings of Machine Learning Research*, pp. 486–489. PMLR, 2020. URL <http://proceedings.mlr.press/v120/yang20a.html>.
- Fujimoto, S., van Hoof, H., and Meger, D. Addressing function approximation error in actor-critic methods. In Dy, J. G. and Krause, A. (eds.), *Proceedings of the 35th International Conference on Machine Learning, ICML 2018, Stockholm, Sweden, July 10-15, 2018*, volume 80 of *Proceedings of Machine Learning Research*, pp. 1582–1591. PMLR, 2018. URL <http://proceedings.mlr.press/v80/fujimoto18a.html>.
- Fujimoto, S., Meger, D., Precup, D., Nachum, O., and Gu, S. S. Why should I trust you, bellman? the bellman error is a poor replacement for value error. In Chaudhuri, K., Jegelka, S., Song, L., Szepesvári, C., Niu, G., and Sabato, S. (eds.), *International Conference on Machine Learning, ICML 2022, 17-23 July 2022, Baltimore, Maryland, USA*, volume 162 of *Proceedings of Machine Learning Research*, pp. 6918–6943. PMLR, 2022. URL <https://proceedings.mlr.press/v162/fujimoto22a.html>.
- Fujita, Y. and Maeda, S. Clipped action policy gradient. In Dy, J. G. and Krause, A. (eds.), *Proceedings of the 35th International Conference on Machine Learning, ICML 2018, Stockholm, Sweden, July 10-15, 2018*, volume 80 of *Proceedings of Machine Learning Research*, pp. 1592–1601. PMLR, 2018. URL <http://proceedings.mlr.press/v80/fujita18a.html>.
- Greensmith, E., Bartlett, P. L., and Baxter, J. Variance reduction techniques for gradient estimates in reinforcement learning. In Dietterich, T. G., Becker, S., and Ghahramani,

- Z. (eds.), *Advances in Neural Information Processing Systems 14 [Neural Information Processing Systems: Natural and Synthetic, NIPS 2001, December 3-8, 2001, Vancouver, British Columbia, Canada]*, pp. 1507–1514. MIT Press, 2001. URL <https://proceedings.neurips.cc/paper/2001/hash/584b98aac2ddd59ee2cf19ca4ccb75e-Abstract.html>.
- Gu, S., Lillicrap, T., Turner, R. E., Ghahramani, Z., Schölkopf, B., and Levine, S. Interpolated policy gradient: Merging on-policy and off-policy gradient estimation for deep reinforcement learning. In Guyon, I., von Luxburg, U., Bengio, S., Wallach, H. M., Fergus, R., Vishwanathan, S. V. N., and Garnett, R. (eds.), *Advances in Neural Information Processing Systems 30: Annual Conference on Neural Information Processing Systems 2017, December 4-9, 2017, Long Beach, CA, USA*, pp. 3846–3855, 2017a. URL <https://proceedings.neurips.cc/paper/2017/hash/a1d7311f2a312426d710e1c617fcbc8c-Abstract.html>.
- Gu, S., Lillicrap, T. P., Ghahramani, Z., Turner, R. E., and Levine, S. Q-prop: Sample-efficient policy gradient with an off-policy critic. In *5th International Conference on Learning Representations, ICLR 2017, Toulon, France, April 24-26, 2017, Conference Track Proceedings*. OpenReview.net, 2017b. URL <https://openreview.net/forum?id=SJ3rcZcxl>.
- Haarnoja, T., Zhou, A., Abbeel, P., and Levine, S. Soft actor-critic: Off-policy maximum entropy deep reinforcement learning with a stochastic actor. In Dy, J. G. and Krause, A. (eds.), *Proceedings of the 35th International Conference on Machine Learning, ICML 2018, Stockholmsmässan, Stockholm, Sweden, July 10-15, 2018*, volume 80 of *Proceedings of Machine Learning Research*, pp. 1856–1865. PMLR, 2018a. URL <http://proceedings.mlr.press/v80/haarnoja18b.html>.
- Haarnoja, T., Zhou, A., Hartikainen, K., Tucker, G., Ha, S., Tan, J., Kumar, V., Zhu, H., Gupta, A., Abbeel, P., and Levine, S. Soft actor-critic algorithms and applications. *CoRR*, abs/1812.05905, 2018b. URL <http://arxiv.org/abs/1812.05905>.
- Ilyas, A., Engstrom, L., Santurkar, S., Tsipras, D., Janoos, F., Rudolph, L., and Madry, A. A closer look at deep policy gradients. In *8th International Conference on Learning Representations, ICLR 2020, Addis Ababa, Ethiopia, April 26-30, 2020*. OpenReview.net, 2020. URL <https://openreview.net/forum?id=ryxdEkHtPS>.
- Kingma, D. P. and Ba, J. Adam: A method for stochastic optimization. In Bengio, Y. and LeCun, Y. (eds.), *3rd International Conference on Learning Representations, ICLR 2015, San Diego, CA, USA, May 7-9, 2015, Conference Track Proceedings*, 2015. URL <http://arxiv.org/abs/1412.6980>.
- Lillicrap, T. P., Hunt, J. J., Pritzel, A., Heess, N., Erez, T., Tassa, Y., Silver, D., and Wierstra, D. Continuous control with deep reinforcement learning. In Bengio, Y. and LeCun, Y. (eds.), *4th International Conference on Learning Representations, ICLR 2016, San Juan, Puerto Rico, May 2-4, 2016, Conference Track Proceedings*, 2016. URL <http://arxiv.org/abs/1509.02971>.
- Mnih, V., Kavukcuoglu, K., Silver, D., Graves, A., Antonoglou, I., Wierstra, D., and Riedmiller, M. A. Playing atari with deep reinforcement learning. *CoRR*, abs/1312.5602, 2013. URL <http://arxiv.org/abs/1312.5602>.
- Schulman, J., Levine, S., Abbeel, P., Jordan, M. I., and Moritz, P. Trust region policy optimization. In Bach, F. R. and Blei, D. M. (eds.), *Proceedings of the 32nd International Conference on Machine Learning, ICML 2015, Lille, France, 6-11 July 2015*, volume 37 of *JMLR Workshop and Conference Proceedings*, pp. 1889–1897. JMLR.org, 2015. URL <http://proceedings.mlr.press/v37/schulman15.html>.
- Schulman, J., Moritz, P., Levine, S., Jordan, M. I., and Abbeel, P. High-dimensional continuous control using generalized advantage estimation. In Bengio, Y. and LeCun, Y. (eds.), *4th International Conference on Learning Representations, ICLR 2016, San Juan, Puerto Rico, May 2-4, 2016, Conference Track Proceedings*, 2016. URL <http://arxiv.org/abs/1506.02438>.
- Schulman, J., Wolski, F., Dhariwal, P., Radford, A., and Klimov, O. Proximal policy optimization algorithms. *CoRR*, abs/1707.06347, 2017. URL <http://arxiv.org/abs/1707.06347>.
- Silver, D., Lever, G., Heess, N., Degris, T., Wierstra, D., and Riedmiller, M. A. Deterministic policy gradient algorithms. In *Proceedings of the 31th International Conference on Machine Learning, ICML 2014, Beijing, China, 21-26 June 2014*, volume 32 of *JMLR Workshop and Conference Proceedings*, pp. 387–395. JMLR.org, 2014. URL <http://proceedings.mlr.press/v32/silver14.html>.
- Sutton, R. S., McAllester, D. A., Singh, S., and Mansour, Y. Policy gradient methods for reinforcement learning with function approximation. In Solla, S. A., Leen, T. K., and Müller, K. (eds.), *Advances in Neural Information Processing Systems 12, [NIPS Conference, Denver, Colorado, USA, November 29 - December 4, 1999]*, pp. 1057–1063. The MIT Press,

1999. URL <http://papers.nips.cc/paper/1713-policy-gradient-methods-for-reinforcement-learning-with-function-approximation>.

Tessler, C., Tennenholtz, G., and Mannor, S. Distributional policy optimization: An alternative approach for continuous control. In Wallach, H. M., Larochelle, H., Beygelzimer, A., d'Alché-Buc, F., Fox, E. B., and Garnett, R. (eds.), *Advances in Neural Information Processing Systems 32: Annual Conference on Neural Information Processing Systems 2019, NeurIPS 2019, December 8-14, 2019, Vancouver, BC, Canada*, pp. 1350–1360, 2019. URL <https://proceedings.neurips.cc/paper/2019/hash/72da7fd6d1302c0a159f6436d01e9eb0-Abstract.html>.

Todorov, E., Erez, T., and Tassa, Y. Mujoco: A physics engine for model-based control. In *2012 IEEE/RSJ International Conference on Intelligent Robots and Systems, IROS 2012, Vilamoura, Algarve, Portugal, October 7-12, 2012*, pp. 5026–5033. IEEE, 2012. doi: 10.1109/IROS.2012.6386109. URL <https://doi.org/10.1109/IROS.2012.6386109>.

van Hasselt, H. Reinforcement learning in continuous state and action spaces. In Wiering, M. A. and van Otterlo, M. (eds.), *Reinforcement Learning*, volume 12 of *Adaptation, Learning, and Optimization*, pp. 207–251. Springer, 2012. doi: 10.1007/978-3-642-27645-3_7. URL https://doi.org/10.1007/978-3-642-27645-3_7.

van Hasselt, H., Doron, Y., Strub, F., Hessel, M., Sonnerat, N., and Modayil, J. Deep reinforcement learning and the deadly triad. *CoRR*, abs/1812.02648, 2018. URL <http://arxiv.org/abs/1812.02648>.

Weaver, L. and Tao, N. The optimal reward baseline for gradient-based reinforcement learning. In Breese, J. S. and Koller, D. (eds.), *UAI '01: Proceedings of the 17th Conference in Uncertainty in Artificial Intelligence, University of Washington, Seattle, Washington, USA, August 2-5, 2001*, pp. 538–545. Morgan Kaufmann, 2001. URL https://dslpitt.org/uai/displayArticleDetails.jsp?mmnu=1&smnu=2&article_id=141&proceeding_id=17.

Williams, R. J. Simple statistical gradient-following algorithms for connectionist reinforcement learning. *Mach. Learn.*, 8:229–256, 1992. doi: 10.1007/BF00992696. URL <https://doi.org/10.1007/BF00992696>.

A. Optimal Baseline

A.1. Proof of Equation 3

We define gradient components as follows:

$$\begin{aligned} g &= u_\theta(s, a)(Q^\pi(s, a) - b(s)) \\ g_1 &= u_\theta(s, a)Q^\pi(s, a) \\ g_2 &= u_\theta(s, a)b(s) \end{aligned} \quad (23)$$

Note that $g = g_1 - g_2$, therefore,

$$\begin{aligned} \mathbb{V}[g] &= \mathbb{E}_{\rho_\pi, \pi}[(g - \mathbb{E}_{\rho_\pi, \pi}[g])^T(g - \mathbb{E}_{\rho_\pi, \pi}[g])] \\ &= \mathbb{E}_{\rho_\pi, \pi} \left[\left((g_1 - \mathbb{E}_{\rho_\pi, \pi}[g_1]) - (g_2 - \mathbb{E}_{\rho_\pi, \pi}[g_2]) \right)^T \left((g_1 - \mathbb{E}_{\rho_\pi, \pi}[g_1]) - (g_2 - \mathbb{E}_{\rho_\pi, \pi}[g_2]) \right) \right] \\ &= \mathbb{V}[g_1] + \mathbb{V}[g_2] - 2\mathbb{E}_{\rho_\pi, \pi}[(g_1 - \mathbb{E}_{\rho_\pi, \pi}[g_1])^T(g_2 - \mathbb{E}_{\rho_\pi, \pi}[g_2])] \quad \xrightarrow{0} \\ &= \mathbb{V}[g_1] + \mathbb{V}[g_2] - 2\mathbb{E}_{\rho_\pi, \pi}[g_1^T g_2] - 2(\mathbb{E}_{\rho_\pi, \pi}[g_1])^T \mathbb{E}_{\rho_\pi, \pi}[g_2] \quad \xrightarrow{0} \\ &= \mathbb{V}[g_1] + \mathbb{V}[g_2] - 2\mathbb{E}_{\rho_\pi, \pi}[g_1^T g_2] \end{aligned} \quad (24)$$

Given a state s , we can omit the expectation over ρ_π , which is taken on the state space. It turns out to be:

$$\begin{aligned} \mathbb{V}[g|s] &= \mathbb{V}[g_1|s] + \mathbb{V}[g_2|s] - 2\mathbb{E}_\pi[g_1^T g_2|s] \\ &= \mathbb{E}_\pi[u_\theta(s, a)^T u_\theta(s, a)Q^\pi(s, a)^2|s] - \\ &\quad (\mathbb{E}_\pi[u_\theta(s, a)Q^\pi(s, a)|s])^2 + \\ &\quad \mathbb{E}_\pi[u_\theta(s, a)^T u_\theta(s, a)b(s)^2|s] - \\ &\quad 2\mathbb{E}_\pi[u_\theta(s, a)^T u_\theta(s, a)Q^\pi(s, a)b(s)|s] + \end{aligned} \quad (25)$$

In an attempt to minimize this variance, using the fact that $\mathbb{V}[g_1|s]$ doesn't depend on $b(s)$, we can differentiate it w.r.t. b , immediately, we get:

$$b^*(s) = \frac{\mathbb{E}_\pi[u_\theta(s, a)^T u_\theta(s, a)Q^\pi(s, a)|s]}{\mathbb{E}_\pi[u_\theta(s, a)^T u_\theta(s, a)|s]} \quad (26)$$

B. Unified Advantage Estimator

B.1. Proof of Proposition 3.1

For any $n \in \mathbb{N}^+$, we telescope over residual terms

$$\sum_{l=0}^{n-1} \gamma^l \delta_{t+l} = \left(\sum_{l=0}^{n-1} \gamma^l r_{t+l} + \gamma^n \Psi_{t+n} - b_t \right) + \sum_{l=1}^{n-1} \gamma^l (\Psi_{t+l} - b_{t+l}) \quad (27)$$

Since the Ψ is the true appraisal, being either Q^π or V^π , thus the Bellman expectation equation is naturally agreed. Denote $z_t = \Psi_t - b_t$, and move the z_t terms from the lefthand side to the righthand size, by taking the expectation of the both sides, it can be shown that

$$\begin{aligned} \mathbb{E}_\pi[A_t^{(n)}] &= \mathbb{E}_\pi \left[\sum_{l=0}^{n-1} \gamma^l r_{t+l} + \gamma^n \Psi_{t+n} - b_t \right] \\ &= \Psi_t - b_t \\ &= A_t^{\pi, b} \end{aligned} \quad (28)$$

B.2. Proof of Equation 6

$$\begin{aligned}
 \hat{A}_t^{\text{UAE}(\gamma, \lambda)} &= (1 - \lambda)(\hat{A}_t^{(1)} + \lambda\hat{A}_t^{(2)} + \lambda^2\hat{A}_t^{(3)} + \dots) \\
 &= (1 - \lambda)(\delta_t + \lambda(\delta_t + \gamma\delta_{t+1} - \gamma z_{t+1}) + \lambda^2(\delta_t + \gamma\delta_{t+1} - \gamma z_{t+1} + \gamma^2\delta_{t+2} - \gamma^2 z_{t+2}) + \dots) \\
 &= (1 - \lambda)\left((\delta_t(1 + \lambda + \dots) + \gamma\delta_{t+1}(\lambda + \lambda^2 + \dots) + \dots) \right. \\
 &\quad \left. - (\gamma z_{t+1}(\lambda + \lambda^2 + \dots) + \gamma^2 z_{t+2}(\lambda^2 + \lambda^3 + \dots) + \dots)\right) \\
 &= (1 - \lambda)\left(\left(\frac{\delta_t}{1 - \lambda} + (\gamma\lambda)\frac{\delta_{t+1}}{1 - \lambda} + \dots\right) - \left((\gamma\lambda)\frac{z_{t+1}}{1 - \lambda} + (\gamma\lambda)^2\frac{z_{t+2}}{1 - \lambda} + \dots\right)\right) \\
 &= \sum_{l=0}^{\infty} (\gamma\lambda)^l \delta_{t+l} - \sum_{l=1}^{\infty} (\gamma\lambda)^l z_{t+l} \\
 &= \delta_t + \sum_{l=1}^{\infty} (\gamma\lambda)^l (\delta_{t+l} - z_{t+l})
 \end{aligned} \tag{29}$$

C. Learn a Baseline

C.1. Proof of Theorem 4.3

Let π_N be a shorthand for π (we will internally change the notation if necessary), and since $\sup_i D_{\text{TV}}(\pi_i || \pi) < \frac{\epsilon}{4}$ and $\mathbb{E}_{\pi}[|r_{\psi^*}(s, a)|] < \frac{\epsilon}{2}$ for any $s \in \mathcal{S}$, then it follows that

$$\begin{aligned}
 \left| \sum_{i=1}^N \int_{\mathcal{A}} (\pi_i - (1 + r_{\psi^*})\pi_N) Q^{\pi_N} da \right| &\leq \sum_{i=1}^N \left| \int_{\mathcal{A}} (\pi_i - (1 + r_{\psi^*})\pi_N) Q^{\pi_N} da \right| \\
 &\leq \sum_{i=1}^N \int_{\mathcal{A}} |\pi_i - (1 + r_{\psi^*})\pi_N| |Q^{\pi_N}| da \\
 &\leq \frac{C_r}{1 - \gamma} \sum_{i=1}^N \int_{\mathcal{A}} |\pi_i - (1 + r_{\psi^*})\pi_N| da \\
 &\leq \frac{C_r}{1 - \gamma} \sum_{i=1}^N \left(2 \cdot \left(\frac{1}{2} \int_{\mathcal{A}} |\pi_i - \pi_N| da \right) + \int_{\mathcal{A}} \pi_N |r_{\psi^*}| da \right) \\
 &< \frac{C_r}{1 - \gamma} \sum_{i=1}^N \left(2 \frac{\epsilon}{4} + \frac{\epsilon}{2} \right) \\
 &= \frac{C_r}{1 - \gamma} N \epsilon
 \end{aligned} \tag{30}$$

By dividing N from both sides, we have

$$\begin{aligned}
 \frac{C_r}{1-\gamma} \epsilon &\geq \left| \frac{1}{N} \sum_{i=1}^N \int_{\mathcal{A}} (\pi_i - (1+r_{\psi^*})\pi_N) Q^{\pi_N} da \right| \\
 &= \left| \frac{1}{N} \left(\sum_{i=1}^{N-1} \int_{\mathcal{A}} (\pi_i - \pi) Q^{\pi} da - N \mathbb{E}_{\pi} [r_{\psi^*} Q^{\pi}] \right) \right| \\
 &= \left| \frac{1}{N} \left(\sum_{i=1}^{N-1} \mathbb{E}_{\pi_i} [Q^{\pi}] - \mathbb{E}_{\pi} [(N-1 + N r_{\psi^*}) Q^{\pi}] \right) \right| \\
 &= \left| \frac{1}{N} \sum_{i=1}^{N-1} (\mathbb{E}_{\pi_i} [Q^{\pi}] + \mathbb{E}_{\pi} [Q^{\pi}]) - \mathbb{E}_{\pi} [(1+r_{\psi^*}) Q^{\pi}] \right| \\
 &= |\mathbb{E}_{\pi_{\mu}} [Q^{\pi}] - \mathbb{E}_{\pi} [(1+r_{\psi^*}) Q^{\pi}]|
 \end{aligned} \tag{31}$$

where the last equality holds for that given a state s , $\pi_{\mu} = \frac{1}{N} \sum_{i=1}^N \pi_i$. Let $g_{r_{\psi^*}}(s) = \mathbb{E}_{\pi} [\nabla_{\psi} r_{\psi^*} Q^{\pi}]$, then it follows that

$$\begin{aligned}
 |\nabla_{\psi} \mathcal{L}(\psi^*)| &= |\mathbb{E}_{d_{\mu}} \{2 \cdot (\mathbb{E}_{\pi} [(1+r_{\psi^*}) Q^{\pi}] - Q^{\pi}) g_{r_{\psi^*}}(s)\}| \\
 &\leq \mathbb{E}_{(s,a) \sim d_{\mu}} \{2 \cdot |(\mathbb{E}_{\pi} [(1+r_{\psi^*}) Q^{\pi}] - Q^{\pi})| |g_{r_{\psi^*}}(s)|\} \\
 &\leq \mathbb{E}_{s \sim d_{\mu}} \{2 \cdot |(\mathbb{E}_{\pi} [(1+r_{\psi^*}) Q^{\pi}] - \mathbb{E}_{a \sim \pi_{\mu}} [Q^{\pi}])| |g_{r_{\psi^*}}(s)|\} \\
 &\leq \frac{2C_r C_g}{1-\gamma} \epsilon
 \end{aligned} \tag{32}$$

C.2. Proof of Corollary 4.4

By $D_{\text{TV}}^2(p||q) \leq D_{\text{KL}}(p||q)$, we have $\sup_s D_{\text{TV}}(\tilde{\pi}||\pi) < \frac{\sqrt{\epsilon}}{2}$

$$\begin{aligned}
 \mathbb{E}_{d_{\mu}} [(\hat{b}_{\psi^*}^{\tilde{\pi}} - \hat{b}_{\psi^*}^{\pi})^2] &= \mathbb{E}_{d_{\mu}} \left[\left(\int_{\mathcal{A}} (\tilde{\pi} - \pi) (1+r_{\psi^*}) Q^{\pi} da \right)^2 \right] \\
 &= \mathbb{E}_{d_{\mu}} \left[\left| \int_{\mathcal{A}} (\tilde{\pi} - \pi) (1+r_{\psi^*}) Q^{\pi} da \right|^2 \right] \\
 &\leq \mathbb{E}_{d_{\mu}} \left[\left(\int_{\mathcal{A}} |\tilde{\pi} - \pi| (1+r_{\psi^*}) |Q^{\pi}| da \right)^2 \right] \\
 &< \frac{((\tilde{C}+1)C_r)^2}{(1-\gamma)^2} \mathbb{E}_{d_{\mu}} \left[\left(2 \cdot \frac{1}{2} \int_{\mathcal{A}} |\tilde{\pi} - \pi| da \right)^2 \right] \\
 &< \frac{((\tilde{C}+1)C_r)^2}{(1-\gamma)^2} \mathbb{E}_{d_{\mu}} \left[\left(2 \cdot \frac{\sqrt{\epsilon}}{2} \right)^2 \right] \\
 &= \frac{((\tilde{C}+1)C_r)^2}{(1-\gamma)^2} \epsilon
 \end{aligned} \tag{33}$$

And with the fact that $(a+b)^2 \leq 2(a^2+b^2)$, we have that

$$\begin{aligned}
 \mathbb{E}_{d_{\mu}} [(Q_w - \hat{b}_{\psi^*}^{\tilde{\pi}})^2] &= \mathbb{E}_{d_{\mu}} [(Q_w - \hat{b}_{\psi^*}^{\pi} + \hat{b}_{\psi^*}^{\tilde{\pi}} - \hat{b}_{\psi^*}^{\pi})^2] \\
 &\leq 2 \cdot \left(\mathbb{E}_{d_{\mu}} [(Q_w - \hat{b}_{\psi^*}^{\pi})^2] + \mathbb{E}_{d_{\mu}} [(\hat{b}_{\psi^*}^{\tilde{\pi}} - \hat{b}_{\psi^*}^{\pi})^2] \right) \\
 &< 2\mathcal{L}(\psi^*) + \frac{2((\tilde{C}+1)C_r)^2}{(1-\gamma)^2} \epsilon
 \end{aligned} \tag{34}$$

D. Practical Algorithm

D.1. Proof of Lemma 5.1

$$\begin{aligned}\|\mathbb{E}\mathcal{T}^\pi Z_1 - \mathbb{E}\mathcal{T}^\pi Z_2\|_\infty &= \gamma \|\mathbb{E}_{s',a'}[\mathbb{E}Z_1 - \mathbb{E}Z_2]\|_\infty \\ &\leq \gamma \|\mathbb{E}Z_1 - \mathbb{E}Z_2\|_\infty\end{aligned}\quad (35)$$

$$\begin{aligned}\|\mathbb{V}\mathcal{T}^\pi Z_1 - \mathbb{V}\mathcal{T}^\pi Z_2\|_\infty &= \sup_{s,a} |\mathbb{V}\mathcal{T}^\pi Z_1(s,a) - \mathbb{V}\mathcal{T}^\pi Z_2(s,a)| \\ &= \sup_{s,a} |\mathbb{E}[\mathbb{V}\mathcal{T}^\pi Z_1(s,a) - \mathbb{V}\mathcal{T}^\pi Z_2(s,a)]| \\ &= \sup_{s,a} \gamma^2 |\mathbb{E}[\mathbb{V}Z_1(S',A') - \mathbb{V}Z_2(S',A')]| \\ &\leq \sup_{s',a'} \gamma^2 |\mathbb{V}Z_1(s',a') - \mathbb{V}Z_2(s',a')| \\ &= \gamma^2 \|\mathbb{V}Z_1 - \mathbb{V}Z_2\|_\infty\end{aligned}\quad (36)$$

D.2. Proof of Proposition 5.2

Suppose (μ_i, σ_i) , $i = 1, 2$ indexed by 1 is the parameters of the target distribution, and 2 of the learnable distribution. Since σ_1 and σ_2 are constantly equal as σ , it means that both of them are not parameterized, then it immediately follows with the definition of the KL divergence between two normal distributions

$$\begin{aligned}D_{\text{KL}}(\mathcal{N}(\mu_1, \sigma_1), \mathcal{N}(\mu_2(\phi), \sigma_2)) &= \log\left(\frac{\sigma_2}{\sigma_1}\right) + \frac{\sigma_1^2 + (\mu_1 - \mu_2(\phi))^2}{2\sigma_2^2} - \frac{1}{2} \\ &= \log\left(\frac{\sigma}{\sigma}\right) + \frac{\sigma^2}{2\sigma^2} - \frac{1}{2} + \frac{(\mu_1 - \mu_2(\phi))^2}{2\sigma^2} \\ &= \frac{1}{\sigma^2} \text{MSE}(\mu_1, \mu_2(\phi))\end{aligned}\quad (37)$$

D.3. Proof of Equation 18

Suppose the learnable distribution is parameterized as $\mathcal{N}(\mu(\phi), \sigma(\zeta))$. Taking gradient of the KL divergence loss, it can be attained

$$\begin{aligned}\nabla_{(\phi, \sigma)} D_{\text{KL}}(\mathcal{N}(\mu_1, \sigma_1), \mathcal{N}(\mu_2(\phi), \sigma_2(\zeta))) &= -\frac{((\sigma_1^2 - \sigma_2^2(\zeta)) + (\mu_1 - \mu_2(\phi))^2) \nabla_\zeta \sigma_2(\zeta)}{\sigma_2^3(\zeta)} - \frac{(\mu_1 - \mu_2(\phi)) \nabla_\phi \mu_2(\phi)}{\sigma_2^2(\zeta)} \\ &= \Delta\sigma_2 + \Delta\mu_2\end{aligned}\quad (38)$$

In practice, the sampling is involved as transition dynamics evolves, thus the $\mu_1 = r + \gamma \cdot \text{mean}(Z_{\bar{w}}(s', a'))$, and $\sigma_1 = \gamma \cdot \text{stddev}(Z_{\bar{w}}(s', a'))$. And $\mu_2 = \text{mean}(Z_w(s, a))$, and $\sigma_2 = \text{stddev}(Z_w(s, a))$. It is clear that the parameters of the learnable distribution is always chasing for discounted ones of the target distribution.

D.4. Proof of Equation 20

$$\begin{aligned}\nabla_\theta \mathcal{L}_{\text{off-policy}}(\theta) &= \nabla_\theta \mathbb{E}_{s \sim D, a \sim \pi_\theta} [\log \pi_\theta(a|s)(A^+(s, a) - \alpha \log \pi_\theta(a|s) - \log N(s))] \\ &= \mathbb{E}_{s \sim D, a \sim \pi_\theta} [\nabla_\theta \log \pi_\theta(a|s)(A^+(s, a) \\ &\quad - \alpha \log \pi_\theta(a|s) - \log N(s))] - \mathbb{E}_{s \sim D, a \sim \pi_\theta} [\nabla_\theta \log \pi_\theta(a|s) \log N(s)] \\ &\quad + \mathbb{E}_{s \sim D, a \sim \pi_\theta} [\nabla_\theta \log \pi_\theta(a|s)] \\ &= \mathbb{E}_{s \sim D, a \sim \pi_\theta} [\nabla_\theta \log \pi_\theta(a|s)(A^+(s, a) - \alpha \log \pi_\theta(a|s))]\end{aligned}\quad (39)$$

Since that

$$\begin{aligned}
 \mathbb{E}_{s \sim D, a \sim \pi_\theta} [\nabla_\theta \log \pi_\theta(a|s) \log N(s)] &= \int d_{\mathcal{D}}(s) \int \nabla_\theta \pi_\theta(a|s) \log N(s) da ds \\
 &= \int d_{\mathcal{D}}(s) \log N(s) (\nabla_\theta \int \pi_\theta(a|s) da) ds \\
 &= 0
 \end{aligned} \tag{40}$$

and

$$\begin{aligned}
 \mathbb{E}_{s \sim D, a \sim \pi_\theta} [\nabla_\theta \log \pi_\theta(a|s)] &= \int d_{\mathcal{D}}(s) \int \pi_\theta(a|s) \frac{\nabla_\theta \pi_\theta(a|s)}{\pi_\theta(a|s)} da ds \\
 &= \int d_{\mathcal{D}}(s) \int \nabla_\theta \pi_\theta(a|s) da ds \\
 &= \int d_{\mathcal{D}}(s) (\nabla_\theta \int \pi_\theta(a|s) da) ds \\
 &= 0
 \end{aligned} \tag{41}$$

D.5. Proof of Theorem 5.3

Since the limit of the s_k exists for any $s \in \mathcal{S}$, it implies that $\lim_{i \rightarrow \infty} \int_{\mathcal{A}} (\pi_i(a|s) - (1 + r_{\psi^*}(s, a))\pi^*(a|s)) Q^{\pi^*}(s, a) da = 0$. With $|Q^{\pi^*}|$ and $|r_{\psi^*}|$ bounded, we have

$$|(\pi_i - (1 + r_{\psi^*})\pi^*) Q^{\pi^*}| \leq \frac{(2 + C_g)C_\tau}{1 - \gamma} \tag{42}$$

And $\lim_{i \rightarrow \infty} (\pi_i(a|s) - (1 + r_{\psi^*}(s, a))\pi^*(a|s)) Q^{\pi^*}(s, a) = -\pi^*(a|s) r_{\psi^*}(s, a) Q^{\pi^*}(s, a)$, thus by applying Lebesgue bounded convergence theorem, we have that

$$\int_{\mathcal{A}} \pi^*(a|s) r_{\psi^*}(s, a) Q^{\pi^*}(s, a) da = 0 \tag{43}$$

Since the π^* is a deterministic optimal policy, the domain \mathcal{A} can be classified either $\mathcal{A}^0 = \{a | \pi^*(a|s) = 0, a \in \mathcal{A}\}$ or $\mathcal{A} \setminus \mathcal{A}^0$. Equation 43 can be rewritten as

$$Q^* \int_{\mathcal{A} \setminus \mathcal{A}^0} \pi^*(a|s) r_{\psi^*}(s, a) da = 0 \tag{44}$$

where Q^* stands for the maximum action-value. As the π^* is deterministic, then $Q^{\pi^*}(s, a) = Q^*$ for any $a \in \mathcal{A} \setminus \mathcal{A}^0$. Thus it follows

$$\begin{aligned}
 \limsup_{k \rightarrow \infty} A_k^+ &= \limsup_{k \rightarrow \infty} (Q^{\pi_k}(s, a) - b_{\psi_k}(s))^+ \\
 &= \limsup_{k \rightarrow \infty} (Q^{\pi^*}(s, a) - b_{\psi_k}(s))^+ \\
 &= (Q^{\pi^*}(s, a) - \mathbb{E}[(1 + r_{\psi^*}(s, a)) Q^{\pi^*}(s, a)])^+ \\
 &= (Q^{\pi^*}(s, a) - V^{\pi^*}(s) - Q^* \int_{\mathcal{A} \setminus \mathcal{A}^0} \pi^*(a|s) r_{\psi^*}(s, a) da)^+ \\
 &= (Q^{\pi^*}(s, a) - V^{\pi^*}(s))^+ = 0
 \end{aligned} \tag{45}$$

Last equality holds for that $V^{\pi^*}(s) = \max_{a \in \mathcal{A}} Q^{\pi^*}(s, a)$

E. Action Bounds Transformation

The support of Beta distribution is $[0, 1]$, for multivariate case with n dimensions which are mutually independent, it would be n products of $[0, 1]$. In practice, the action bounds doesn't have to fit into this domain, we therefore need to apply a linear transformation upon each dimension to coincide with the actual bound $[m_i, M_i]$, $i = 1, 2, \dots, n$, where m_i is the lower bound, and M_i upper bound. It would be convenient to vectorize those bounds as \mathbf{m} and \mathbf{M} .

Let $\mathbf{x} \in \mathbb{R}^n$ be a Beta-distributed random vector whose density is $f(\mathbf{x}|\mathbf{s})$. It is transformed as a new random vector $\mathbf{a} = x \cdot (\mathbf{M} - \mathbf{m}) + \mathbf{m}$ to be the action executed in the environment, at which product is element-wise. Denote $\mathbf{k} = \mathbf{M} - \mathbf{m}$ and $\mathbf{b} = \mathbf{m}$, its log-likelihood is given by

$$\log \pi(\mathbf{a}|\mathbf{s}) = \log f(\mathbf{x}|\mathbf{s}) - \mathbf{1}^\top \log \mathbf{k} \quad (46)$$

where $\mathbf{1}^\top$ is a n -dimensional vector whose entry is one. Since $\mathbf{1}^\top \log \mathbf{k}$ is a constant, the difference of the log-likelihood π reduces to the that of the original one f , namely

$$\log \tilde{\pi}(\mathbf{a}|\mathbf{s}) - \log \pi(\mathbf{a}|\mathbf{s}) = \log \tilde{f}(\mathbf{x}|\mathbf{s}) - \log f(\mathbf{x}|\mathbf{s}) \quad (47)$$

This invariance is useful especially for the case that the log-likelihood policy gradient is involved e.g. A2C, TRPO and PPO. And it should be noted that only the $f(\mathbf{a}|\mathbf{s})$ is parameterized as $f_\theta(\mathbf{a}|\mathbf{s})$, thus $\pi_\theta(\mathbf{a}|\mathbf{s}) = f_\theta(\mathbf{a}|\mathbf{s})$. We store the transformed action \mathbf{a} and the untransformed log-likelihood $\log f(\mathbf{a}|\mathbf{s})$, which is used in the policy improvement phase, to either calculate the difference of the log-likelihoods (TRPO, PPO) or the log-likelihood only (A2C). By detransforming the action \mathbf{a} to the original one \mathbf{x} , $\tilde{f}(\mathbf{x}|\mathbf{s})$ can be calculated for those aforementioned purposes.

F. Experimental Details

F.1. Figure 2

The counterpart of UAE is the Monte-Carlo estimate, whose return R is estimated by the data of the batch \mathcal{B} , and the advantage is calculated as $A = R - b$.

F.2. Figure 3

- The value baseline is fitted by the Monte-Carlo return.
- The variance is estimated upon the data of the batch \mathcal{B} with length T

$$\hat{V}(\pi_\theta) = \frac{1}{T} \sum_{(s,a) \sim \mathcal{B}} \|u_\theta(s, a)\|_2^2 (Q_w(s, a) - \hat{b}_\psi^{\pi_\theta}(s))^2 \quad (48)$$

where the score function is calculated element-wisely.

F.3. Figure 4

We borrow the metrics from (Fujimoto et al., 2022) with modifications. The mean absolute error (MAE), namely generalization error, is performed on the subset \mathcal{D}_e of the test data $\mathcal{D}_{\text{test}}$ (will be introduced later)

$$\frac{1}{|\mathcal{D}_e|} \sum_{(s,a) \sim \mathcal{D}_e} |Q_w(s, a) - Q^\pi(s, a)| \quad (49)$$

where the test data $\mathcal{D}_{\text{test}}$ is collected by executing current policy π in the environment with 50000 steps, and \mathcal{D}_e is formed as the uniformly sampled data (size = 1000) from the test data. For each (s, a) in the \mathcal{D}_e , the true action-value function Q^π is approximated by the Monte-Carlo estimate with 100 episodes, each of which has a timelimit 1000 (which means each episode cannot exceed that limit). The root mean squared error (RMSE), namely prediction error, is performed on the data of the batch \mathcal{B} (size = 2048)

$$\frac{1}{|\mathcal{B}|} \sum_{(s,a) \sim \mathcal{B}} \sqrt{(Q_w(s, a) - (r + \gamma Q_w(s', a')))^2} \quad (50)$$

The Q_w all of above is the mean value of the learned distribution $Q_w(s, a) = \mathbb{E}[Z_w(s, a)]$.

F.4. Figure 5

The positive advantage A^+ is estimated on the uniformly sampled data (size = 25000) from the replay buffer \mathcal{D} , by taking the mean and max value.

E.5. Figure 6

We perform all algorithms on the MuJoCo tasks with v3 version, except PPO, which is on the v2 version. The reason is that we observe the OpenAI Baselines implementation doesn't learn on the v3 version tasks at all, to make the results comparable, and respect the originality of the specific algorithm implementation, we have to make this compromise.

G. Implementation Details

G.1. Advantage Interpolation

We introduce another interpolating parameter ν for advantage estimate over \mathcal{B} before the policy improvement. Since we evaluate at each environment step, we expect a good quality that the expected value $Q_w = \mathbb{E}[Z_w]$ would achieve.

$$\hat{A} = (1 - \nu)A^{\text{UAE}} + \nu(Q_w - b_\psi) \tag{51}$$

G.2. Normalization

Like PPO, we adopt observation normalization, reward normalization, and advantage normalization (batch level), as it is beneficial to stabilize the behavior of the neural network, thus enable fast learning. Unlike PPO, we minimize the code-level optimization, such as network initialization, learning rate decay, gradient clipping etc.

H. Hyperparameters

Hyperparameter	Value
optimizer	Adam (Kingma & Ba, 2015)
learning rate	3×10^{-4}
size of replay buffer \mathcal{D}	1000000
size of mini batch from \mathcal{B}	256
size of mini batch from \mathcal{D}	256
discounted factor γ	0.99
UAE λ	0.95
target smoothing parameter τ	$5e - 3$
policy interpolating parameter ω	0.7
advantage interpolating parameter ν	0.3
temperature α	0.05
on-policy learner	PPO
clipping parameter ε	0.2
size of batch \mathcal{B}	2048
epochs per batch	10
baseline updates	12
num samples	64
on-policy learner	A2C
size of batch \mathcal{B}	256
epochs per batch	1
baseline updates	4
num samples	32
on-policy learner	TRPO
max kl	0.1
damping	0.1
size of batch \mathcal{B}	4096
epochs per batch	1
baseline updates	12
num samples	64

Table 2. Hyperparameters of DPO

- Only half of the num samples is used to train the baseline, whereas full samples for obtaining the baseline.
- Learning rate is kept constant for all networks.

I. Additional Experiments

I.1. Variants of DPO

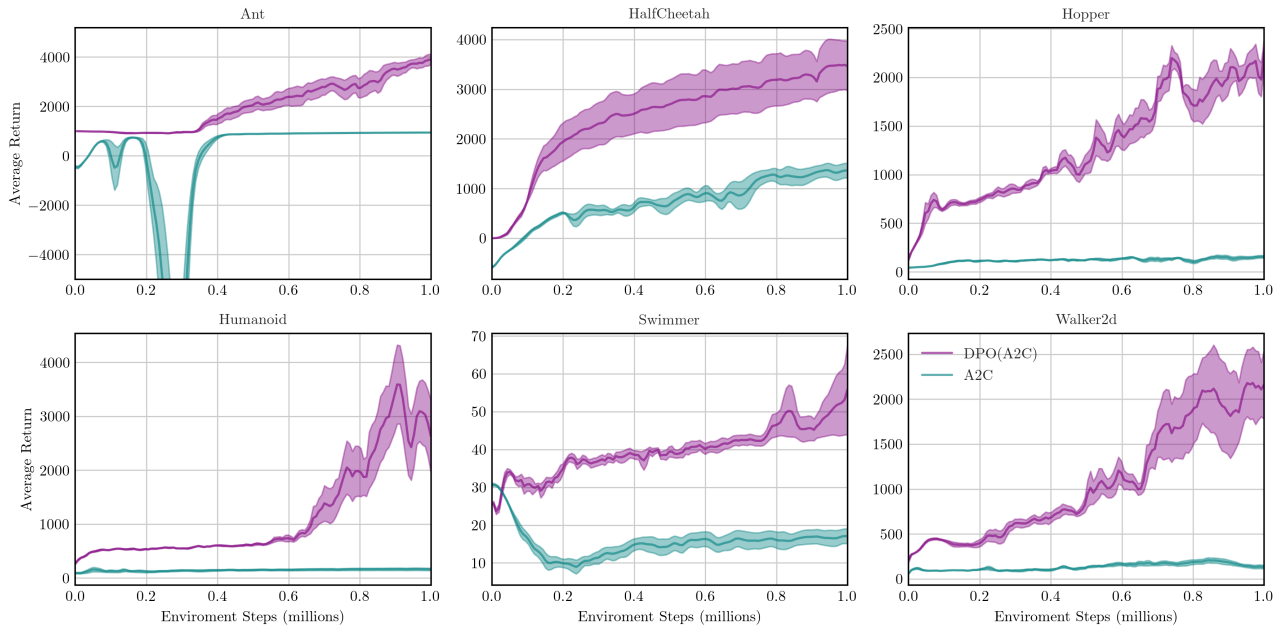


Figure 7. Comparison between DPO(A2C) and A2C, averaged over 5 random seeds and shaded with standard error.

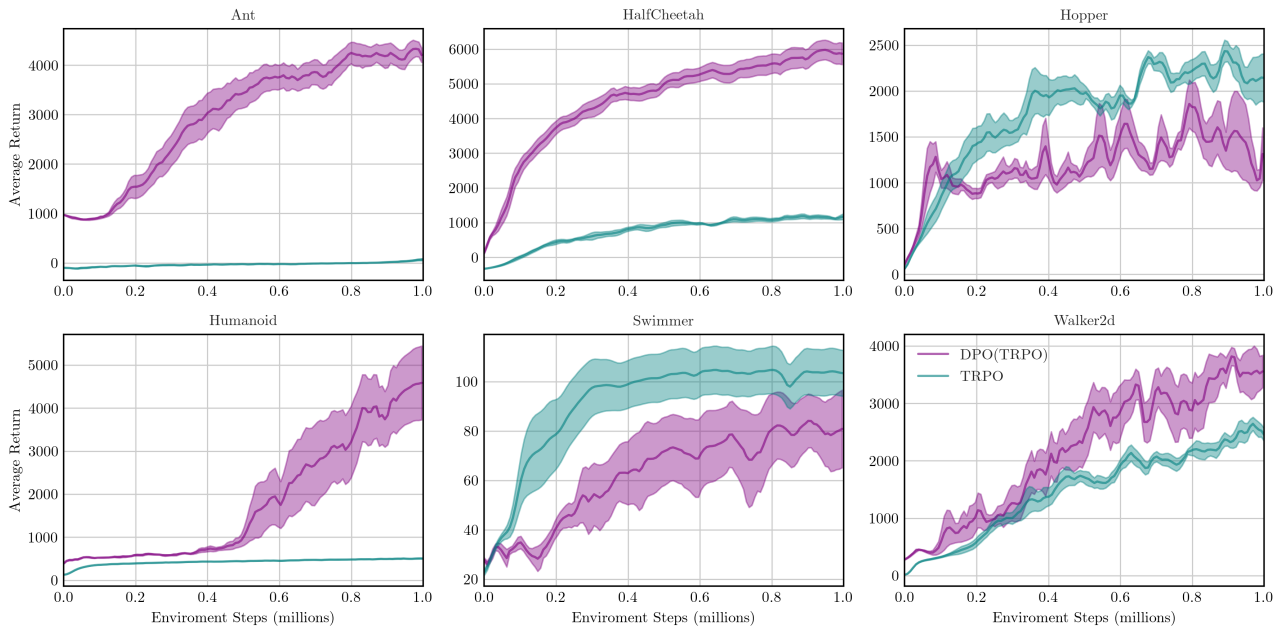


Figure 8. Comparison between DPO(TRPO) and TRPO, averaged over 5 random seeds and shaded with standard error.

I.2. Effects of Main Parameters

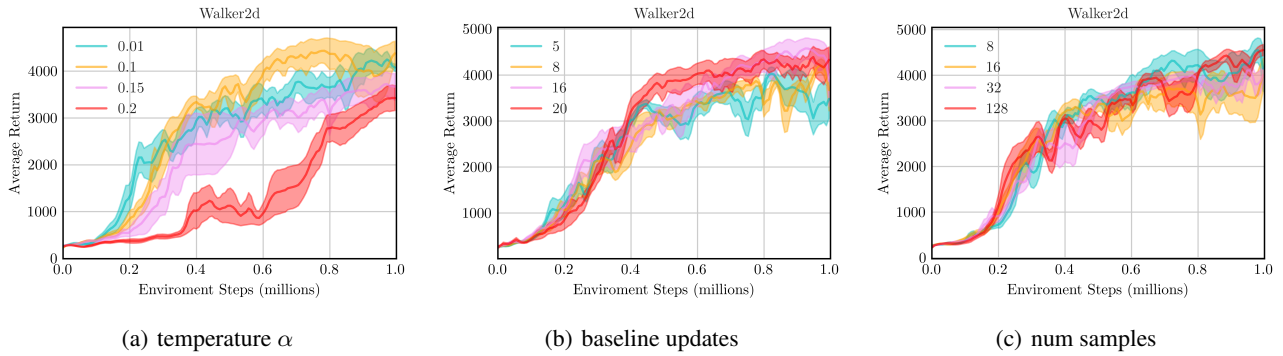


Figure 9. Varying levels of different parameters for DPO: temperature α , baseline updates, and num samples.

While our algorithm is insensitive to the baseline updates and num samples, for computation’s sake, we would choose moderate values for them. In contrast, the algorithm is indeed sensitive to the temperature parameter, the larger which would be, the more fluctuations would occur. Choosing an appropriate α without being too large would be advisable.